Available online at www.sciencedirect.com
SCIENCE DIRECT®
Journal of Catalysis 224 (2004) 449–462
JOURNAL OF CATALYSIS
www.elsevier.com/locate/jcat

Kinetics, mechanism, and the influence of H_2 on the CO oxidation reaction on a Au/TiO_2 catalyst

B. Schumacher,[a] Y. Denkwitz,[a] V. Plzak,[b] M. Kinne,[a] and R.J. Behm [a,*]

[a] *Department of Surface Chemistry and Catalysis, University Ulm, D-89069 Ulm, Germany*
[b] *Center for Solar Energy and Hydrogen Research, Helmholtzstr. 8, D-89081 Ulm, Germany*

Received 15 September 2003; revised 24 February 2004; accepted 25 February 2004

Available online 20 April 2004

Abstract

We present results of a kinetic and in situ IR spectroscopic study, including isotope-labeling experiments, on the CO oxidation behavior over a highly active Au/TiO_2 catalyst prepared via a novel synthesis procedure, and on the effect of H_2 on the CO adsorption/reaction characteristics under conditions relevant for CO removal from CO-contaminated feed gases for polymer electrolyte fuel cells (PEFCs) via preferential CO oxidation (PROX). The results show that (i) H_2 affects the CO oxidation, most probably by competing hydrogen adsorption on the Au nanoparticles and reaction with oxygen, which results in a significantly higher CO reaction order, that (ii) formate and carbonate species formed during the reaction represent (reaction inhibiting) side products, but do not take part in the reaction as reaction intermediate, at least not under present reaction conditions, and that (iii) the formation of formate and carbonate species is inhibited during reaction in a H_2-rich atmosphere. This is tentatively attributed to the decomposition of these species by reaction with H_2O, which is formed in the process gas upon H_2 oxidation.

Keywords: Kinetic measurements; IR spectroscopy; DRIFTS; Isotope-labeling experiments; CO oxidation; Preferential CO oxidation; Reaction kinetics; Adsorption; Carbonate formation; Deactivation; Au/TiO_2 catalyst

1. Introduction

Highly disperse, metal oxide-supported Au catalysts have been found to be extremely active for various oxidation and hydrogenation reactions, in particular for CO oxidation [1–4]. These studies have shown that in addition to the catalyst dispersion, the procedure for catalyst preparation and conditioning and the nature of the oxide support play an important role, and it was distinguished between "active," easily reducible supports and less active ("inert"), stable oxides [5]. One of the most active support materials is TiO_2. On Au/TiO_2 catalysts the reaction was observed even at temperatures as low as 90 K [6]. Highly active Au/TiO_2 catalysts are commonly prepared by coprecipitation (CP) or by deposition–precipitation (DP), followed by calcination in air at temperatures between 200 and 400 °C [7–12]. Recent work in our group has shown that supported Au catalysts prepared via a DP procedure using rather different process parameters, followed by calcination at 400 °C or a reductive treatment at 200 °C, exhibit a similar or even higher activity [13].

Following previous studies on different oxide-supported Au catalysts [5,13–18] we investigated the CO oxidation reaction and in particular the influence of H_2 on this reaction on Au/TiO_2 catalysts prepared along this route. In order to unravel the effect of H_2 on the CO oxidation characteristics and on the interaction of CO with the Au/TiO_2 catalyst comparative measurements were carried out in H_2-free and H_2-rich gas mixtures. The interest in the effect of H_2 arises from the potential application of these catalysts for the removal of CO from CO-contaminated, H_2-rich feed gases for low-temperature polymer electrolyte fuel cells (PEFCs) generated by steam reforming and/or partial oxidation of hydrocarbons or methanol [19–22]. Therefore, the reaction and adsorption experiments were performed under adsorption/reaction conditions relevant for processing of H_2-rich feed gases for PEFCs. This includes CO partial pressures up to 1.5 kPa, together with high H_2 contents in the H_2-rich at-

* Corresponding author.
E-mail address: juergen.behm@chemie.uni-ulm.de (R.J. Behm).

0021-9517/$ – see front matter
doi:10.1016/j.jcat.2004.02.036

mosphere, a low O_2 excess, and adsorption/reaction temperatures around 80 °C, which is a typical working temperature of PEFCs.

Because of the widely varying results on the catalytic activity of catalysts depending on the catalyst preparation and pretreatment procedures we are particularly interested in comparing our results with existing data obtained on these catalysts prepared via different routes.

A first report on the preparation, conditioning, and stability of these Au/TiO_2 catalysts was published recently in [23]. In the present paper we will focus on three different aspects:

(i) on the kinetics of the CO oxidation reaction on these catalysts, and on the influence of H_2 on the reaction kinetics,
(ii) on the interaction of these catalysts with CO, both in an inert gas mixture and under reaction conditions in a H_2-free as well as in a H_2-rich atmosphere, and
(iii) on questions regarding the reaction mechanism, and the influence of H_2 on the reaction mechanism.

In the first part of the results (Section 3.1) we report and discuss kinetic measurements, focusing on the influence of the CO and O_2 partial pressures under present reaction conditions, and on the effect of H_2 on the reaction kinetics. Despite the numerous studies on the activity of differently prepared (and pretreated) Au/TiO_2 catalysts for CO oxidation (see [3,4,10] and references therein), more detailed catalyst kinetic studies, performed under differential reaction conditions, are scarce so far. This is particularly true for reaction conditions relevant for processing PEFC feed gases as described above [8,24–26]. The influence of H_2 on the CO oxidation kinetics had been investigated so far only in conversion measurements, performed on a 1 wt% Au/TiO_2 catalyst [27].

The following Section 3.2 concentrates on the interaction of CO with the Au/TiO_2 catalyst in H_2-free and H_2-rich atmospheres (see above), in the presence of O_2 ("reactive atmosphere") and in the absence of O_2 ("inert atmosphere"), which was studied by IR. This topic had been investigated already in numerous previous IR studies, in particular by the group of Boccuzzi et al., but also by other groups (see [28] and the above reviews), using Au/TiO_2 catalysts prepared via different routes and both inert and reactive (O_2 containing) atmospheres. These studies unanimously concluded that CO is adsorbed on the Au nanoparticles and, if investigated, that carbonate-like and carboxylic species are formed on the surface. The influence of H_2 on the interaction between the CO and the Au/TiO_2 catalyst has not been investigated so far. In order to elucidate the effect of the catalyst-conditioning procedure, IR measurements were performed both on calcined catalysts and on reductively treated catalysts.

The last Section 3.3 aims at mechanistic aspects for CO oxidation on these Au/TiO_2 catalysts, using isotope-exchange experiments. Here it was tested whether oxygen exchange is possible with these catalysts when flowing O_2 over the catalyst, either in a dilute O_2 atmosphere or in a CO-containing atmosphere, during CO oxidation. A previous study using a 3 wt% Au/TiO_2 catalyst prepared in a different way, by supporting a Au–phosphine complex on titanium hydroxide, had not shown any isotope scrambling of O_2, neither during interaction of a mixture of $^{16}O_2$ and $^{18}O_2$ with that catalyst nor during reaction with CO [29], which supports the assumption of O_2^- as a reactive species during CO oxidation, indicative of molecular O_2 adsorption for that type of catalyst. The ratio of the different CO_2 isotopomers formed by reaction of $C^{16}O$ with $^{16}O_2$ and $^{18}O_2$ allows further conclusions on the reaction mechanism.

2. Experimental

2.1. Preparation and pretreatment of the catalyst

Three different catalysts were used in this study. They were prepared in the same way but with different Au loadings (Au/TiO_2(A) and Au/TiO_2(C), 2.4 wt% Au; catalyst Au/TiO_2(B), 4.5 wt% Au), via a deposition precipitation (DP) procedure which was reported in detail elsewhere [23]. In short, an aqueous solution of $HAuCl_4$ was added to a suspension of annealed TiO_2 powder (Anatase, Sachtleben VP9413/3, annealed in air at about 700 °C for 30 min, TiO_2 particle sizes 21–25 nm). The resulting precipitate was filtered, carefully washed to remove residual Na and Cl [30], and then dried over night at room temperature under vacuum. Prior to the experiments the samples were conditioned either by the conventional procedure, by calcining in 10% O_2 in N_2 at 400 °C for 30 min [1,8], or via a reductive conditioning process, involving 45 min annealing in 10% H_2 in N_2 at 200 °C [23], and then cooled down in N_2 to the respective reaction/adsorption temperature. After these treatments the Au particle sizes were around 2.5–3 nm after calcination and about 1.8 nm after reductive treatment, respectively, [23].

2.2. Kinetic measurements

Kinetic measurements were performed at atmospheric pressure in a quartz tube micro reactor (i.d. 4 mm) located in a ceramic tube oven and under differential reaction conditions, with typically 100 mg catalyst powder (catalyst bed length 5–8 mm). In order to limit the conversion to values typically between 5 and 20%, in some cases for the lowest concentrations also slightly higher values, the catalyst samples were diluted with α-Al_2O_3, which is not active for CO oxidation under the present conditions. Reactions were carried out with a flux of 60 N ml/min (space velocity 41,000 h^{-1}) at 80 °C in two different atmospheres, in a H_2-free atmosphere with different amounts of CO and O_2 and N_2 as balance, and in a H_2-rich atmosphere with different amounts of CO and O_2, 75 kPa H_2, and again N_2 as balance. Kinetic data were acquired after 85 min reaction time. Influent and effluent gases were analyzed by on-line

gas chromatography (Dani GC 86.10HT). High-purity reaction gases (CO 4.7, O_2 5.0, H_2 5.0, N_2 6.0 from Westphalen) were used. Evaluation of the Weisz criterion showed the absence of mass-transport-related problems [31]. For further details, in particular on the determination of activities and selectivities, see [32].

2.3. Infrared investigations

In situ IR investigations were performed in a DRIFTS (diffuse reflectance infrared spectroscopy) configuration with a Magna 560 spectrometer from Nicolet, equipped with a MCT narrow band detector and a commercial in situ reaction cell unit from Harricks (HV-DR2). This setup allows measurements in a continuous flow of gas mixtures, equal to those used in the kinetic studies, and at elevated temperatures. Typically 400–600 scans (acquisition time ~ 4 min) at a nominal resolution of 8 cm^{-1} were added for one spectrum. Intensities were evaluated in Kubelka–Munk units, which are linearly related to the adsorbate concentration [33]. Prior to the experiments background spectra were recorded on the freshly conditioned catalyst at reaction temperature under a flow of pure nitrogen, which were used for normalization. Finally, spectral contributions of gas phase CO were removed by subtracting a reference spectrum recorded over an inert carrier under similar conditions. For further details see [15].

2.4. Experiments with isotope-labeled gases

These experiments were performed in a plug-flow reactor similar to that used for the kinetic measurements, which was connected to an ion-molecule-reaction mass spectrometer (IMR-MS) for educt/product detection (Atomica IMR-MS SP89). This method, which relies on the ionization of reaction gases by slow noble gas ions (Xe^+ or Kr^+), is less susceptible to fragmentation than the commonly used mass spectrometers involving electron-induced ionization [34]. In addition, gases with ionization energies larger than the electron affinity of Xe^+ or Kr^+, such as N_2 and H_2, cannot be ionized, which allows quantitative detection of CO in the presence of N_2. Important for the present studies is that because of the low fragmentation probability the quantitative detection of CO is possible also in the presence of CO_2 without being affected by fragmentation of CO_2. $C^{18}O$ and $^{18}O_2$ were used as dilute mixtures (1.25% $C^{18}O$ in N_2 (6.0) and 1.25% $^{18}O_2$ in N_2 (6.0), Linde), in some experiments they were mixed with nonlabeled gases.

3. Results and discussion

3.1. Reaction kinetics

We first studied the influence of the CO partial pressure at a constant ratio of CO partial pressure to O_2 partial pressure, $p_{CO} = p_{O_2}$, which is equivalent to an oxygen excess of $\lambda = 2$. The variation of the normalized CO oxidation rate (normalized to 1 g of Au) is illustrated for two different catalysts (Au/TiO_2(A) and Au/TiO_2(B)) in Fig. 1a. TOF numbers can be derived from these rates via the catalyst dispersion (Au/TiO_2(A), 31.6% dispersion, and Au/TiO_2(B), 35.4% dispersion after calcination at 400 °C); in the present case a rate of 10^{-3} mol g_{Au} s^{-1} corresponds to TOF numbers of 0.62 for catalyst Au/TiO_2(A) and 0.56 for catalyst Au/TiO_2(B), respectively. In both reaction atmospheres the reaction rates decay continuously with decreasing CO partial pressure. (Note that because of the constant λ in these measurements the O_2 partial pressure is reduced in the same way.) As seen in the double logarithmic plot in Fig. 1a, the logarithmic reaction rates are proportional to the logarithmic CO partial pressure over the entire pressure range investigated (0.03–2 kPa), indicating a constant reaction order in a power-law description of the reaction rates over the entire partial pressure range. In the present case, with constant λ, the slope of the resulting lines yields the overall reaction order α^{λ}_{CO}, which in this description is related to the reaction orders for CO and O_2, α_{CO} and α_{O_2}, respectively, by $\alpha^{\lambda}_{CO} = \alpha_{CO} + \alpha_{O_2}$ [32].

Table 1
Reaction orders for CO oxidation over catalysts Au/TiO_2(A) and Au/TiO_2(B) (see Fig. 1)

Catalyst	AuTi(A)		AuTi(B)
Reaction atmosphere	H_2 rich	H_2 free	H_2 rich
α_{CO}	0.82 ± 0.16	0.34 ± 0.07	1.01 ± 0.15
α_{O_2}	0.36 ± 0.02	0.32 ± 0.03	0.39 ± 0.02

The two data sets for the reaction in H_2-free atmosphere (open symbols) were obtained for the same catalyst (Au/TiO_2(A)), but in a different sequence of measurements, one with increasing partial pressure (△), the other with decreasing partial pressures (▽). The data sets obtained in H_2-rich atmosphere (filled symbols) represent results obtained on two different catalysts, Au/TiO_2(A) (▼) and Au/TiO_2(B) (●). The respective reaction orders are collected in Table 1.

Comparing the results obtained in the absence of H_2 (open symbols) with those measured in a H_2-rich atmosphere (filled symbols), it is obvious that the pressure dependence is much more pronounced for CO oxidation in the H_2-rich atmosphere, with a slope of $\alpha^{\lambda}_{CO} = 1.21$ (filled points) compared to $\alpha^{\lambda}_{CO} = 0.66$ in a H_2-free gas mixture. For $p_{CO} < 1$ kPa the CO oxidation rate is generally lower in the H_2-rich atmosphere than in the absence of H_2. The difference, however, decreases with increasing partial pressures.

The reaction order α_{CO} was determined by keeping the O_2 partial pressure constant at 0.1 kPa and varying the partial pressure of CO (Fig. 1b). Also in this case the data lie on a straight line, both for reaction in a H_2-free (open symbols) and in a H_2-rich atmosphere (filled symbols). The slope is again considerably higher in the latter case, and the rates coincide at the highest pressures (1–2 kPa). The absolute

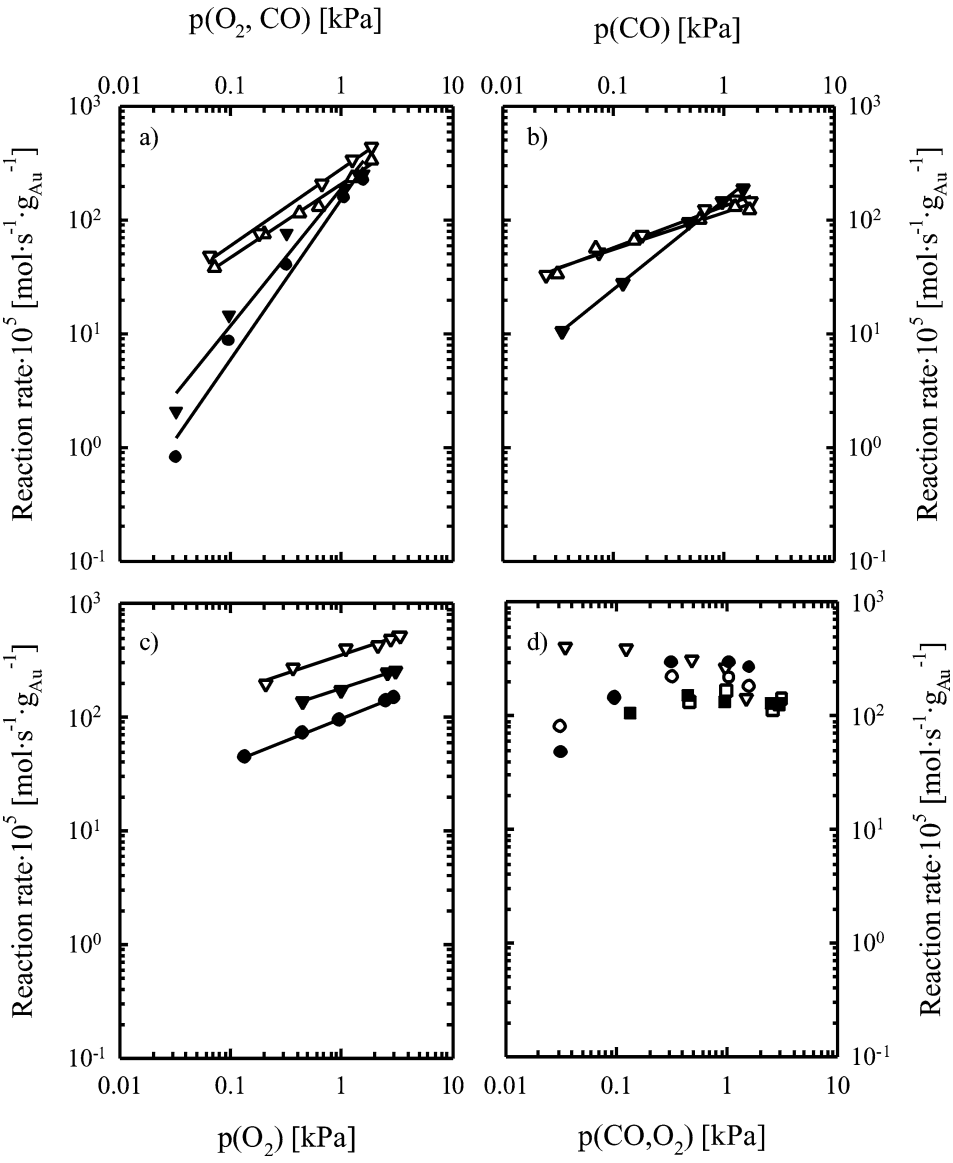

Fig. 1. Determination of the reaction orders (overall reaction order α_{CO}^{λ}, reaction order for CO α_{CO}, reaction order for O_2 α_{O_2}) and the selectivity for CO oxidation in H_2-free and in H_2-rich atmospheres for two different catalysts, Au/TiO_2(A) and Au/TiO_2(B) (diluted catalyst, oxidative pretreatment, 80 °C reaction temperature). If not mentioned differently, the measurements were performed from high to low pressures. (a) Overall reaction order α_{CO}^{λ} for $\lambda = 2(p_{CO} = p_{O_2})$: Au/TiO_2(A) in H_2-free atmosphere measured from low to high (△, $\alpha_{CO}^{\lambda} = 0.64$) and from high to low partial pressures (▽, $\alpha_{CO}^{\lambda} = 0.69$); $AuTiO_2$(A) in H_2-rich atmosphere (▼, $\alpha_{CO}^{\lambda} = 1.21$); Au/TiO_2(B) in H_2-rich atmosphere (●, $\alpha_{CO}^{\lambda} = 1.40$). (b) CO reaction order α_{CO} ($p_{O_2} = 0.1$ kPa, p_{CO} variable): Au/TiO_2(A) in H_2-free atmosphere, measured from low to high CO partial pressures (△, $\alpha_{CO} = 0.32$) and measured from high to low partial pressures (▽, $\alpha_{CO} = 0.37$); Au/TiO_2(A) in H_2-rich atmosphere (▼, $\alpha_{CO} = 0.78$). (c) O_2 reaction order α_{O_2} ($p_{CO} = 1$ kPa, p_{O_2} variable): Au/TiO_2(A) in H_2-free atmosphere (▽, $\alpha_{O_2} = 0.32$); Au/TiO_2(A) in H_2-rich atmosphere (▼, $\alpha_{O_2} = 0.36$); Au/TiO_2(B) in H_2-rich atmosphere (●, $\alpha_{O_2} = 0.39$). (d) H_2 oxidation activity during the above reactions in H_2-rich atmosphere for catalysts Au/TiO_2(A) and Au/TiO_2(B): Au/TiO_2(A), α_{CO}^{λ} (○); Au/TiO_2(B), α_{CO}^{λ} (●); Au/TiO_2(A), α_{CO} (▽), Au/TiO_2(A), α_{O_2} (□), Au/TiO_2(B), α_{O_2} (■).

values agree well with those in Fig. 1a for comparable conditions ($p_{CO} = p_{O_2} = 0.1$ kPa). The respective values for the reaction order α_{CO} are summarized in Table 1.

Next, the reaction order α_{O_2} was determined by keeping the CO partial pressure constant at 1 kPa and varying the partial pressure of O_2 (Fig. 1c). Again the data fall on a straight line, both for reaction in a H_2-free (open symbols) and in a H_2-rich atmosphere (filled symbols). The absolute values agree well with those in Fig. 1a for comparable conditions ($p_{CO} = p_{O_2} = 1$ kPa). In this case, however, the reaction order α_{O_2} is not sensitive to the reaction atmosphere, with $\alpha_{O_2} = 0.32$ in H_2-free atmosphere and $\alpha_{O_2} = 0.36$ in H_2-rich atmosphere (catalyst Au/TiO_2(A)). As expected for the relatively high CO partial pressures the effect of the reaction atmosphere is rather small, though the rates are still higher in the absence of H_2 than in the presence of H_2.

Using the reaction orders α_{CO}^{λ} and α_{O_2}, we also determined α_{CO} via the relation $\alpha_{CO}^{\lambda} = \alpha_{CO} + \alpha_{O_2}$. The resulting

Table 2
Kinetic parameters for CO oxidation over supported Au/TiO_2 catalysts and relevant reaction parameters

Catalyst loading (wt%)	Preparation	Catalyst condition	d_{Au} (nm)	α_{CO}	p_{CO}; p_{O_2} (kPa)	α_{O_2}	p_{CO}, p_{O_2} (kPa)	T (K)	E^* (kJ/mol)	Ref.
H_2-free atmosphere										
3.3	DP	C	3	0.05	0.5–20; 20	0.24	1; 0.7–20	273	34	[8]
2.3	IM	HTR/C/LTR	30	0.24[a]	2–25; 5	0.4[b]	5; 2–19	313–333	9.6	[24]
1	IM	HTR/C/LTR	30	~ 0.4[c]	n.r.; 5	~ 0[c]	5; n.r.	273–313	29	[25]
2	IM	HTR, C	30	0.45	0.5–2; 4	0.19	0.3–2, 4	320	32	[61]
1	IM	C		0.25	n.r.	0.41	n.r.	n.r.	16.3	[29]
1	IM			0.2	3.67–16.5; 3.67	0.46	3.67–17.0, 3.67	293	16.3	[27]
2.4	DP	LTR,C	2.7	0.34	0.02–2; 0.1	0.32	1; 0.2–3	353	–	Present work
H_2-rich atmosphere										
2.4	DP	C	2.7	0.82	0.02–2; 0.1	0.36	1; 0.1–3	353	25	Present work

Abbreviations: DP, deposition–precipitation; IM, impregnation; LTR, low-temperature reduction; HTR, high-temperature reduction; C, calcination.
[a] 0.6 at 353 K, 0.5 at 313 K, and lower pressures.
[b] α_{O_2} may be somewhat lower at lower pressures.
[c] The difference in reaction orders between [24] and [25] was explained by these authors by changes in the 2.3% Au/TiO_2 catalyst due to stronger deactivation before the data were collected [25].

values for α_{CO} (see Table 1) are very close to those determined directly from the data in Fig. 1b, at very different O_2 partial pressures. This indicates that there are no major changes in the reaction mechanism within the pressure range used in these experiments.

For comparison of the reaction orders determined here in a H_2-free atmosphere values determined in previous kinetic studies as well as the relevant reaction conditions are collected in Table 2. For reaction at 0 °C on a 3.3 wt% Au/TiO_2 catalyst Haruta et al. derived a CO reaction order near zero ($\alpha_{CO} = 0.05$), an O_2 reaction order of $\alpha_{O_2} = 0.24$ and an activation energy of 34 kJ/mol [8]. Vannice and co-workers reported reaction orders of $\alpha_{CO} = 0.4$ for reaction between 0 and 20 °C, which increased to $\alpha_{CO} = 0.56$ at 40 °C, and an O_2 reaction order of $\alpha_{O_2} \approx 0$ for reaction at 0–20 °C ($\alpha_{O_2} \approx 0.1$ at 40 °C) [25]. It should be noted that the catalysts used in the latter study, which were prepared via an impregnation procedure, exhibited much larger Au particles (particle size 30 nm) than the catalysts used by the Haruta group (2.5–5 nm, as visible on the TEM image in that paper), which were prepared via a DP procedure worked out by this group. For reaction on a 2% Au/TiO_2 catalyst prepared by an incipient wetness technique Ossipoff and Cant determined reaction orders of $\alpha_{CO} = 0.45$ and $\alpha_{O_2} = 0.19$ under comparable conditions as well as an activation energy of 32 kJ/mol [26]. Using a different procedure for catalyst preparation, by grafting a Au–phosphine complex onto TiO_2 support material, Choudhary et al. derived reaction orders of $\alpha_{CO} = 0.2$ and $\alpha_{O_2} = 0.46$ at 20 °C for a 1 wt% Au/TiO_2 catalyst, and an activation energy of 16.3 kJ/mol [27]. Almost identical values were reported also by Liu et al. for a similar type catalyst [29].

The main results of this comparison are that (i) there is a considerable spread in the data and that (ii) in all studies both the CO and the O_2 reaction orders are slightly positive, between 0.05 and 0.46. At least part of the spread in the data can be explained by the very different reaction conditions ($CO:O_2$ ratio, absolute partial pressures, reaction temperature), as, e.g., in the case of the data in Ref. [8]. Furthermore, regardless of the catalyst preparation, etc., the reaction appears to be limited by the respective reactants and not by a lack of reactive sites, at least under reaction conditions considered in these studies. The reaction orders determined here for CO oxidation in a H_2-free atmosphere on a DP-prepared catalyst fit well to the previously published data. The same holds true for the absolute rates and TOF numbers obtained here, which agree well with those obtained for highly active Au/TiO_2 catalysts prepared via conventional procedures under comparable conditions [27].

The results obtained in a H_2-rich atmosphere differ significantly. Here the CO reaction order is more than twice as high as in the absence of H_2, while that for O_2 is little affected by the presence of H_2. An earlier study of the same reaction over Au/Fe_2O_3 in our laboratory, which was performed under similar reaction conditions, gave a considerably lower value for the CO reaction order, $\alpha_{CO} = 0.55$, while the O_2 reaction order was of similar magnitude ($\alpha_{O_2} = 0.27$) [35]. Additional kinetic data are rare and do not contain information on details such as reaction orders. Torres Sanchez et al. had shown that CO can easily be oxidized over a Au/MnO_x catalyst in a H_2 feed stream ($p_{CO} = p_{O_2} = 1$ kPa, rest H_2) at temperatures of 50–100 °C, but that the CO conversion decreases slightly at higher temperatures (120 °C) [36]. This was attributed to increasing O_2 consumption by H_2 oxidation [36]. A reduction in the CO oxidation activity over Au/TiO_2 in the presence of H_2 by about one-third, from 0.9 to 0.6 mmol/s g_{Au}, can be calculated from the data in [27], which were obtained under not very different reaction conditions (80 °C, $p_{CO} \approx 2$ kPa, $p_{H_2} = 48$ kPa, $\lambda = 4$). A comparison of the PROX activity of different metal oxide-supported Au catalysts (Au/γ-Al_2O_3, Au/Co_3O_4, Au/CeO_2, Au/Fe_2O_3, Au/Ni_2O_3, $Au/Mg(OH)_2$, Au/TiO_2, etc.) at a single gas composition ($p_{CO} = p_{O_2} =$ 1 kPa) by Schubert et al. [13] revealed a considerable vari-

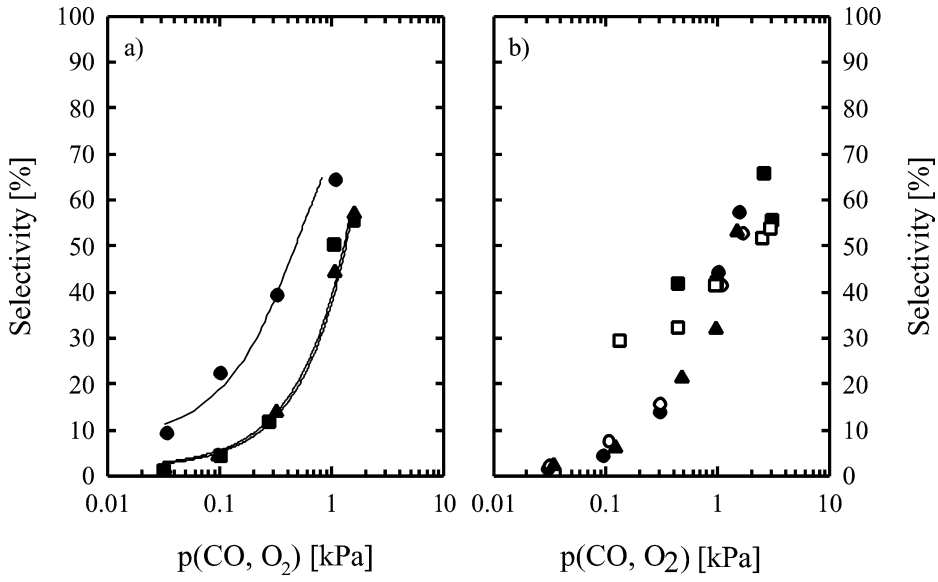

Fig. 2. (a) Selectivity for CO oxidation during the reaction in H_2-rich atmosphere for catalyst Au/TiO_2(A) at different temperatures (40 °C (●), 60 °C (■), 80 °C (▲), $\lambda = 2$). (b) Selectivity during the reactions in Fig. 1 in H_2-rich atmosphere for catalysts Au/TiO_2(A) and Au/TiO_2(B): Au/TiO_2(A) α_{CO}^{λ} (●); Au/TiO_2(B) α_{CO}^{λ} (○); Au/TiO_2(A) α_{CO} (▲); Au/TiO_2(A) α_{O_2} (■); Au/TiO_2(B) α_{O_2} (□) (experimental conditions as in Fig. 1).

ation in activity and selectivity. Likewise, Grisel et al. had reported that the presence of H_2 in the reactant flow had a slightly negative effect on the CO oxidation activity at room temperature over Au/MnO_x/Al_2O_3, but a considerable positive effect for Au/MgO/Al_2O_3 (p_{H_2}:p_{CO}:p_{O_2} = 4:2:1, atmospheric pressure) [37].

Next, Figs. 1d and 2b illustrate the behavior of the activity for H_2 oxidation (Fig. 1d) and the selectivity (Fig. 2b), respectively, in the measurements in a H_2-rich atmosphere. The selectivity is defined by the amount of O_2 consumed for CO oxidation, divided by the total amount of O_2 consumed, and calculated from the balance between CO_2 formation and O_2 consumption [32]. (It should be noted that this is only correct as long as the H_2 level is not affected by any other reactions such as the water-gas-shift (WGS) reaction ($CO + H_2O \leftrightarrow CO_2 + H_2$) or the methanation reaction ($CO + 3H_2 \leftrightarrow CH_4 + H_2O$), which appears justified based on previous measurements of the forward WGS reaction on a Au/TiO_2 catalyst under comparable conditions by Sakurai et al. [38].) As can be seen in Fig. 2b the selectivity depends strongly on the CO partial pressure, decaying from almost 70% at $p_{CO} \geqslant 1$ kPa to a few percent at CO partial pressures < 0.1 kPa. The absolute values of the selectivity fit well to data reported by Choudhary et al. [27], who determined a selectivity of 73% during selective CO oxidation over Au/TiO_2 in a CO:H_2:O_2 mixture of 1:50:2, i.e., at $\lambda = 4$ and $p_{CO} \approx 2$ kPa at 80 °C reaction temperature. A strong dependence of the selectivity on the CO partial pressure at constant λ was reported also for the PROX reaction over Au/Fe_2O_3 [35]. Interestingly, in both cases the pronounced changes in selectivity with CO partial pressure are mainly due to the change in CO oxidation activity, while the H_2 oxidation rate is little affected. These results lead to the conclusions that (i) the reactive sites for H_2 oxidation are not or at least not to a significant extent blocked by the increasing CO coverage and/or that (ii) the reactive oxygen species are not significantly depleted by the CO oxidation reaction. The first conclusion holds true if H_2 activation/dissociation is rate limiting, the second one if O_2 activation/dissociation is rate determining.

Finally, we estimated the activation energies for CO oxidation under these conditions from the kinetic measurements performed at 40, 60, and 80 °C at different CO partial pressures and constant $\lambda = 2$ in H_2-rich gas ($p_{H_2} = 75$ kPa). For CO partial pressures between 0.3 and 2 kPa we obtained values of 25 ± 8 kJ/mol. At lower CO partial pressures, 0.1 and 0.03 kPa, the activation energy decayed to 7 ± 6 and 0 ± 6 kJ/mol, respectively. The higher value agrees well with those reported previously for highly active Au/TiO_2 catalysts and comparable reaction conditions [8,25,29]; for the low CO partial pressures reference values do not exist. The selectivities obtained in these measurements at different CO partial pressures are plotted in Fig. 2a. (The values for 80 °C are included also in Fig. 2b.) While there is not much difference for reaction between 80 and 60 °C, the selectivities are significantly higher at 40 °C, reaching 64% at 1 kPa CO (50 and 40% at 60 and 80 °C, respectively). Also at these lower temperatures the change in selectivity is mostly caused by the change in CO oxidation, while the H_2 oxidation rate is much less affected.

3.2. Infrared investigations

The kinetic studies have shown an increase in CO oxidation rate for higher CO partial pressures at constant λ. In order to deduce whether this increase of the rate is accompanied by a similar increase in CO_{ad} coverage or other

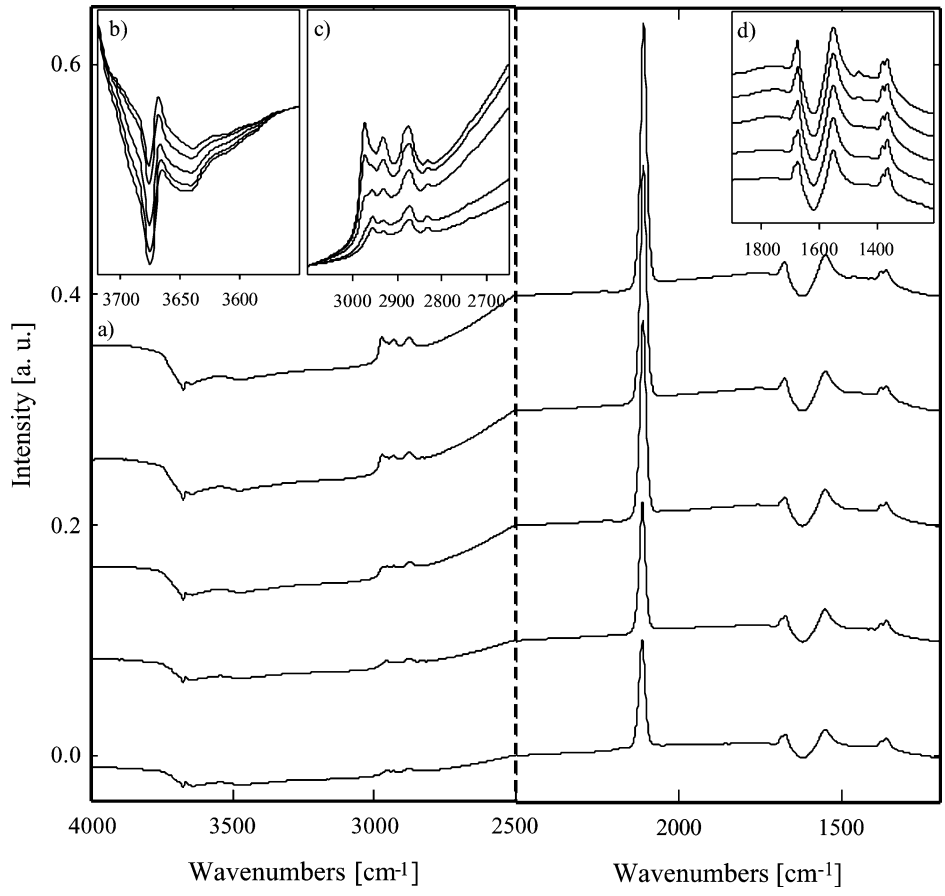

Fig. 3. IR spectra recorded upon adsorption of CO from H_2-free gas mixtures containing increasing amounts of CO in N_2 on the catalyst Au/TiO_2(A) (undiluted catalyst; reductive conditioning). (a) Complete spectra, (b) enlarged detail spectra of the spectral range characteristic for OH groups (on the support), (c) enlarged detail spectra of the formate region, and (d) enlarged detail spectra of the carbonate region. From bottom to top (inset (c) top to bottom): 0.05 kPa CO, 0.1 kPa CO, 0.5 kPa CO, 1.0 kPa CO, 1.5 kPa CO.

changes in the adlayer, we investigated the respective adlayers resulting under different conditions by in situ DRIFTS. This was done in both H_2-free and H_2-rich dilute CO atmospheres, respectively, and in O_2-containing reactive gas mixtures at 80 °C (Figs. 3, 5, 6, 7). Prior to the DRIFTS measurements the catalysts were conditioned either via the reductive treatment or via calcination as described in Section 2, and then cooled down in a flow of N_2. It turned out, however, that the characteristic features and trends in the DRIFT spectra did not depend on the pretreatment. The only exception was a weak peak in the carbonate region, at 1445 cm^{-1}, which appeared during CO adsorption in a H_2-rich atmosphere on a calcined catalyst, but not on a reductively pretreated Au/TiO_2 catalyst. The spectra presented in Figs. 3 and 5 were acquired after a reductive pretreatment, those in Figs. 6 and 7 after oxidative pretreatment.

3.2.1. CO adsorption in H_2-free atmosphere

Spectra recorded in a dilute CO atmosphere, with different amounts of CO in N_2, are presented in Fig. 3. Due to an initial change of the reflectivity after the admission of CO (color changes due to partial reduction of the TiO_2 support) the background spectra did not fit perfectly the CO adsorption spectra. Therefore, the background subtraction had to be done separately for two different spectral regions. Accordingly, differences between different background-corrected spectra are not caused by the initial TiO_2 support modification, but reflect real changes in the adlayer. The spectra obtained upon adsorption from CO/N_2 mixtures are dominated by the absorption peak of adsorbed CO. As expected for CO adsorption on Au nanoparticles; i.e., in agreement with previous observations for CO adsorption on other supported Au catalysts [15,25,27,39,40] and on massive Au surfaces [41,42], only linearly adsorbed CO is observed. The vibrational frequency is almost independent of the CO partial pressure (Fig. 3a, from bottom to top), with only a slight red shift from 2112 cm^{-1} at 0.05 kPa CO to 2108 cm^{-1} at 1.5 kPa CO partial pressure. The increase in intensity with increasing CO partial pressure and the frequency shift with increasing C–O absorption intensity are plotted in Fig. 4. A similar behavior of the C–O vibration, with a frequency shift from 2111 to 2104 cm^{-1} upon a CO partial pressure increase from 0.05 to 1.0 kPa, was observed also for CO adsorption on Au/Fe_2O_3 [15] and on massive Au, from 2129 cm^{-1} at 1.33×10^{-4} kPa CO to 2106 cm^{-1} at atmospheric pressure [41]. This chemical shift, which is op-

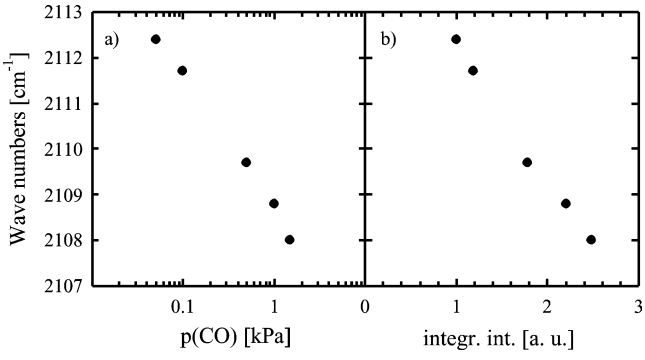

Fig. 4. (a) Frequency shift of the C–O stretch vibration with increasing CO partial pressure upon CO adsorption from H_2-free gas mixtures containing increasing amounts of CO in N_2 (see Fig. 3). (b) Frequency shift with increasing peak intensity (data from part (a)).

posite to the behavior generally observed on transition and noble metal surfaces [43], had been explained by the lack of backdonation from Au d-electrons into the $2\pi^*$ orbital of adsorbed CO, so that the Au–CO bond is dominated by electron donation from the 5σ orbital of the CO molecule, which is slightly antibonding for the C–O bond, to the metal [41]. With increasing CO coverage this effect becomes weaker, leading to a weakening of the C–O bond. In contrast to Bollinger and Vannice we did not see a second peak at 2071 cm^{-1} emerge, which they observed during room temperature CO adsorption ($p_{CO} = 5$ kPa) [25], or of a peak at 2183 cm^{-1} as reported by Haruta et al., which was attributed to CO adsorption on Ti^{4+} sites.

In addition to the C–O vibration signal the spectra exhibit weak, but characteristic, absorption peaks also in the spectral ranges 1350–1700 cm^{-1} (carbonate, carboxylate, and formate species), 2800–3000 cm^{-1} (C–H vibration of formates), and around 3630 cm^{-1} (O–H vibrations) [8,25, 40,44]. In the "carbonate/carboxylate region" (detail spectra see Fig. 3d), characteristic absorption lines are visible at 1672, 1552, 1381, and 1363 cm^{-1}. (After oxidative pretreatment an additional weak peak at 1445 cm^{-1} appears at all CO partial pressures.) In previous studies peaks at 1690 and 1585 cm^{-1} had been assigned to bidentate species on the support [25,45]. Liao et al. distinguished between bridging carbonate (bound to two Ti ions) with frequencies around 1725 cm^{-1} on TiO_2 and bidentate carbonates (bound to a single Ti ion) with frequencies around 1560 cm^{-1} [46]. A peak at 1440 cm^{-1} was assigned to monodentate carbonate [40,46] or free carbonate [25,46]. Vibrations between 1330 and 1370 cm^{-1} had been assigned to COO symmetric stretch frequencies of monodentate (1330 cm^{-1}) and bidentate (1370 cm^{-1}) carbonates as well as formates (1370 cm^{-1}) on the TiO_2 support [13,25,40,44,46,47]. Bond and Thompson had proposed that these species are formed by reaction of a CO molecule adsorbed on a Au particle ("Au^0–CO") with a hydroxyl group adsorbed either on a support cation or on a peripheral ionic Au species, e.g., a Au^{III} ion ("periphery mechanism") [48]. In their model the hydroxyl group is recovered during CO oxidation when two carboxylate ions are oxidized by a superoxide ion. This explanation agrees with the observation that the intensity of the carbonate/carboxylate peaks does not increase with CO partial pressure. It should be noted that adsorbed OH species are present on TiO_2 even after calcination at 500 °C [49].

The proposed interaction of CO with OH_{ad} on peripheral sites agrees well with the evolution of the OH peak with increasing CO partial pressure (enlarged detail spectra see Fig. 3b). The negative peak in the spectra of the O–H stretch frequency at 3677 cm^{-1} fits excellently to OH adsorbed on pure TiO_2, which was reported to have a characteristic absorption band at 3676 cm^{-1} [50]. The negative peak in the spectra indicates a decreasing amount of these species in a CO/N_2 atmosphere compared to that in pure N_2. A chemical interaction or even reaction with adsorbed CO changes the chemical state of the OH group and therefore also the frequency of the O–H stretch vibration, resulting in a positive peak at a somewhat different frequency. The red shift of the new vibration points to a weakening of the O–H bond in the new OH_{ad} species due to interaction/reaction with CO_{ad}.

The intensity of the positive O–H peak does not change with the CO partial pressure in the gas mixture, which fits well to the constant intensity of the carboxylate species. In contrast, the intensity of the negative peak increases with higher CO concentrations, indicating that the consumption of the OH groups is caused not only by the formation of the carbonate/carboxylate species, but also via another reaction path. This is confirmed in the detail spectra in Fig. 3c, which show the continuous growth of characteristic peaks in the formate region, at 2833, 2873, 2931, and 2955 cm^{-1} [25,44]. These peaks had been assigned to C–H stretch vibrations in formates adsorbed on the anatase support [25]. In addition, starting at partial pressures of 0.5 kPa a new peak appears at 2972 cm^{-1}, whose origin has not yet been clarified. This feature grows continuously with CO partial pressure (and adsorption time), in good agreement with the continuous consumption of OH species indicated by the behavior of the negative peak at 3677 cm^{-1}.

3.2.2. CO adsorption in H_2-rich atmosphere

For CO adsorption from a CO/H_2 atmosphere the results are very different. Since the DRIFT spectra showed slow modifications in their overall shape over a significant time span, we present spectra recorded at three different CO partial pressures after 2 min (Fig. 5a) and the temporal evolution of spectra in 0.5 kPa CO in H_2/N_2 (Fig. 5b). As before, background removal was performed in the two regions above and below 2500 cm^{-1} separately. The C–O stretch vibration is slightly red-shifted compared to a H_2-free atmosphere, from about 2110 to 2107 cm^{-1}. This peak increases in intensity, but does not shift with CO partial pressure (Fig. 5a). With increasing adsorption time at 0.5 kPa this peak decreases and is replaced by an asymmetric peak at 2032 cm^{-1}, which includes a shoulder around 1985 cm^{-1} and possibly a second one around 1930 cm^{-1} (Fig. 5b). A comparable peak at 2055 cm^{-1}, with a shoulder at 1990 cm^{-1}, had been re-

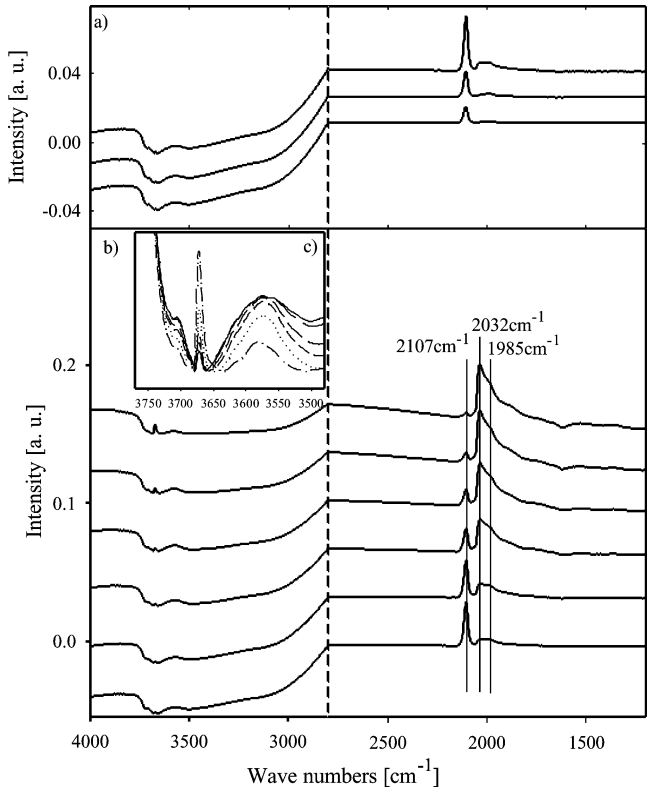

Fig. 5. DRIFT spectra recorded upon adsorption of CO from H_2-rich gas mixtures containing different amounts of CO in 75 kPa H_2/rest N_2 (on the catalyst Au/TiO_2(A) (undiluted catalyst; reductive conditioning). (a) Pressure dependence (bottom to top): 0.05 kPa CO, 0.1 kPa CO, 0.5 kPa CO; spectra taken after 2 min. (b) Complete spectra, and (c) (detail spectra between 3770 and 3480 cm^{-1}) show the temporal development of the spectra during adsorption from 0.5 kPa CO (from bottom to top in (b) and in (c) at 3675 cm^{-1}, from top to bottom at in (c) at 3570 cm^{-1}: 2, 7, 30, 60, 120, and 240 min).

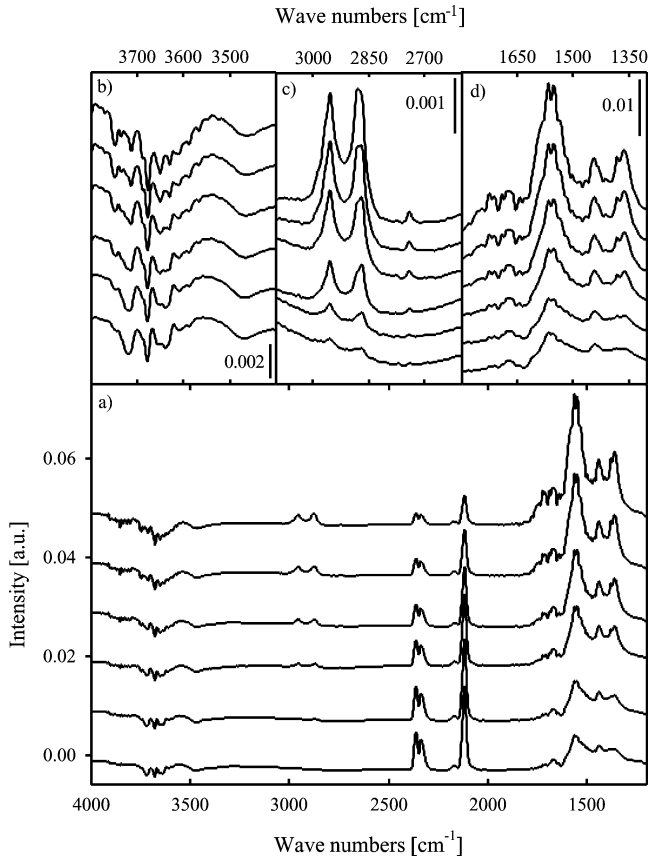

Fig. 6. Sequence of DRIFT spectra recorded during CO oxidation at 80 °C over Au/TiO_2(A) in H_2 free atmosphere (1 kPa CO, 1 kPa O_2, rest N_2, catalyst diluted 1:5 with α-Al_2O_3, calcined at 400 °C). (a) Complete spectra, (b), (c), and (d) enlarged detail spectra of the spectral ranges characteristic for O–H vibrations (b), C–H vibrations in formates (c), and COO vibrations in formates and carbonates (d), respectively. The spectra were recorded after (from bottom to top) 5, 10, 30, 60, 120, and 240 min reaction time.

ported by Boccuzzi et al. for CO adsorption on a Au/TiO_2 sample that was reduced with H_2 at 255 °C before adsorption, in addition to the "normal" peak at 2100 cm^{-1} [51]. On the other hand, this new feature was not observed for CO adsorption from a similar H_2-rich atmosphere on Au/Fe_2O_3 [17]. Boccuzzi et al. explained their findings by a reduction of the support due to reaction with H_2 and a resulting transfer of negative charge to the gold particles, which leads to an increased backdonation and hence to a weakening of the C–O bond, in agreement with the observed peak shift. A charge transfer from TiO_2 to Au nanoparticles has indeed been reported by Jakob et al. [52] when exposing TiO_2 nanoparticles to UV radiation and bringing the resulting, partly reduced, colored TiO_2 nanoparticles into contact with Au nanoparticles. The detail spectra in the inset (Fig. 5c) show a significant rise of the OH peak at 3775 cm^{-1} with increasing adsorption time, indicating that TiO_2 reduction takes place under present conditions. Other possible explanations for the shift in C–O frequency include interactions between H_{ad} and CO_{ad} species coadsorbed on the Au nanoparticles, or a H_{ad}-induced decrease in the steady-state CO coverage. In all three cases, however, one would expect a continuous shift in the C–O frequency and not a new peak at a fixed frequency, as it is observed experimentally. The latter fits better to a distinctly different new CO_{ad} species as expected, e.g., for a compound like H–Au–CO adsorption complex, similar to reports for H_2/CO coadsorption on Ni(100) [53,54], or for a severe, H_2-induced restructuring of the Au nanoparticles. Equally, Bollinger et al. report a weak signal at 2062 cm^{-1} upon CO adsorption on a Au/TiO_2 catalyst pretreated by low-temperature reduction as a last step, which disappears again upon O_2 addition [25]. Finally, we note that neither formates nor carbonate/carboxylate species are formed in the presence of H_2.

3.2.3. CO oxidation in a H_2-free atmosphere

The evolution of adsorbed species with increasing reaction time during CO oxidation in a H_2-free atmosphere (1 kPa CO, 1 kPa O_2, rest N_2) is illustrated in Fig. 6. In this case background removal could be done for the complete spectra. The spectra show linearly adsorbed CO with a frequency of 2118 cm^{-1} as a dominant CO peak and a small feature at 2173 cm^{-1} (Fig. 6a). The C–O stretch frequency

at 2118 cm^{-1} is blue-shifted by about 8 cm^{-1} compared to CO adsorption in the absence of O_2. A similar blue shift of the CO_{ad} vibration in the presence of O_2 was observed by numerous groups [1,25,27]. It was attributed to a coverage effect, a reduction in steady-state CO coverage because of the oxidation reaction. Considering the small CO_{ad} coverage effects observed in the present study, however, we favor contributions from coadsorbed species, e.g., oxygen species coadsorbed on the Au particles, as explanation. The second feature, at 2173 cm^{-1}, was attributed to CO adsorbed on Ti^{4+} [6]. In addition, the spectra exhibit signals characteristic for gas-phase CO_2 at 2361 and 2338 cm^{-1}, and a number of features in the OH, formate, and carbonate regions, which will be described in more detail below. With increasing reaction time the signals of adsorbed CO and CO_2 decay continuously. In contrast to the CO coverage-dependent shifts observed upon CO adsorption from the inert CO/N_2 mixture, the frequency of the C–O vibration remains practically constant. This behavior can be explained by an increasing blocking of the CO adsorption sites, i.e., of the Au nanoparticle surface by the growing formate and carbonate adspecies, which reduces the total amount of adsorbed CO, but leaves the local coverage unchanged.

In the formate region the spectra exhibit two major peaks at $\sim$ 2875 and 2953 cm^{-1} (detail spectra see Fig. 6c). The peak around 2875 cm^{-1} consists of two hardly resolved peaks at 2883 and 2870 cm^{-1}. Furthermore, after 30 min a small peak at 2742 cm^{-1} develops. The peaks at 2953 and 2870 cm^{-1} are identical to those observed upon CO adsorption from the CO/N_2 atmosphere, while the peak at 2742 cm^{-1} is blue-shifted by 10 cm^{-1} compared to that in the latter spectra. Similar as for CO adsorption in a H_2-free atmosphere OH groups adsorbed on the support are removed by carboxylate/carbonate, as evidenced by the negative peak at 3676 cm^{-1}; i.e., the support is depleted by OH groups during the reaction.

The peaks in the carbonate region (detail spectra Fig. 6d), between 1350 and 1700 cm^{-1}, are much more pronounced and structured than those observed for CO adsorption in a CO/N_2 atmosphere (Fig. 3). The main peaks in this region are a band between 1500 and 1620 cm^{-1}, which exhibits several weak maxima and shoulders. In addition, peaks at 1360, 1380, 1440, and $\sim$ 1700 cm^{-1} are found. As noted before peaks at 1690 and 1585 cm^{-1} had been assigned previously to the asymmetric stretch vibration of bridged/bidentate carbonate species on the support [25], a peak at 1440 cm^{-1} to monodentate carbonate or free carbonate [25,40,46], and vibrations between 1300 and 1370 cm^{-1} to the symmetric stretch vibrations of different carbonates and of formate species [40,44,46]. The antisymmetric stretch vibration of formates on TiO_2, which are assumed by those authors to be in a bridging configuration, was identified at about 1555 cm^{-1} [46,47].

Similar effects upon changing to reaction conditions, in particular a blue shift of the C–O stretch vibration in the presence of O_2, were reported by Bollinger and Vannice [25], Boccuzzi, Haruta, and co-workers [1,55], or by Liu et al. [29].

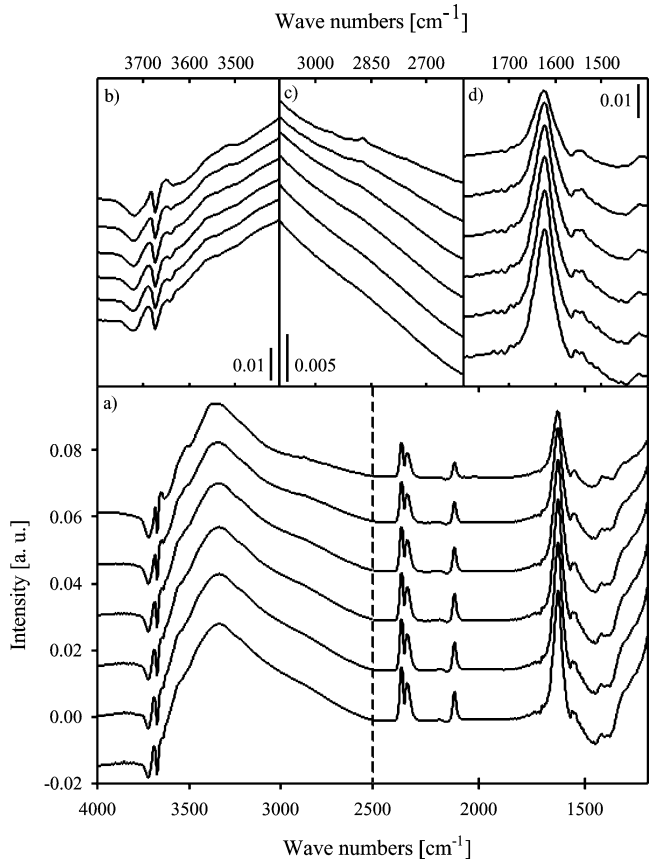

Fig. 7. Sequence of DRIFT spectra recorded during CO oxidation at 80 °C over Au/TiO_2(A) in H_2-rich idealized reformate (1 kPa CO, 1 kPa O_2, 75 kPa H_2, rest N_2, catalyst diluted 1:5 with α-Al_2O_3, calcined at 400 °C). (a) Complete spectra, (b), (c), and (d) enlarged detail spectra of the spectral ranges characteristic for O–H vibrations (b), C–H vibrations in formates (c), and COO vibrations in formates and carbonates (d), respectively. The spectra were recorded after (from bottom to top) 5, 10, 30, 60, 120, and 240 min reaction time.

In our preceding report on the deactivation behavior and long-term stability of this catalyst we had shown that the decreasing amount of adsorbed CO is correlated with a significant decay of the reaction rate [23]. The continuous growth of the carbonate-like species—the intensities of the related IR absorption signals are still growing even after 20 h of reaction time—may be one or perhaps even the dominant reason for the deactivation of the catalyst. Similar observations and conclusions were reported also for CO oxidation in a H_2-rich atmosphere over Au/Fe_2O_3 [17,56]. This will be discussed in more detail in the next paragraph.

3.2.4. CO oxidation in a H_2-rich atmosphere

As in the previous cases the spectral region of the C–O stretch vibration is dominated by a pronounced peak of linearly adsorbed CO, which appears here at 2112 cm^{-1}. Similar to CO oxidation in a H_2-free atmosphere, it does not change its position with time (Fig. 7a). Different from CO adsorption from a H_2-rich atmosphere, however, the

highly asymmetric peak at 2032 cm^{-1} (Fig. 5b) does not develop. A satellite at 2143 cm^{-1} likely results from gaseous CO, which was not perfectly removed by the CO gas-phase subtraction. With increasing reaction time the CO signal decreases in intensity (Fig. 7a), though the decay is less pronounced than that observed in a H_2-free atmosphere (Fig. 6a).

The other spectral areas are dominated by the pronounced signals of the oxidation products CO_2 (2361 and 2338 cm^{-1}) and H_2O, where the latter includes the strong signal of the HOH mode of adsorbed water at 1623 cm^{-1} [40] and the O–H vibration between 2500 and 3200 cm^{-1}. As expected, the latter is much more pronounced (see Fig. 7a) than during reaction in a H_2-free atmosphere (Fig. 6a). With increasing reaction time all of these signals lose considerably in intensity. Similar to CO adsorption in a H_2-rich atmosphere (Fig. 5), formate formation does not seem to play an important role. A weak peak developing at 2874 cm^{-1} (Fig. 7c) is comparable in intensity to that formed upon oxidation in H_2-free atmosphere.

The carbonate region exhibits weak negative signals at $\sim$ 1380, 1440, and 1550/1585 cm^{-1} in addition to the dominant water peak. The negative signals correspond exactly to the (positive) carbonate signals observed upon reaction in a H_2-free atmosphere. We therefore explain them by a reaction-induced decomposition of small amounts of carbonates which had been present at the beginning of the reaction.

The decay in IR intensity and the deactivation of the catalyst must be related to the accumulation of water on the catalyst. A TPD spectrum recorded from a Au/TiO_2 catalyst that had been operating in a H_2-rich atmosphere for 900 min showed H_2O as the only desorbing species (spectrum not shown). We, therefore, assume that a considerable part of the general decrease in intensity in the spectra in Fig. 7a is caused by a change in reflectivity with increasing reaction time. This proposal is supported also by the fact that the decrease in intensity is about equal for all peaks.

The reaction behavior of the Au/TiO_2 catalyst in a H_2-rich atmosphere is very different from that of Au/Fe_2O_3 catalysts [56]. On the latter the reaction leads to a pronounced growth of carbonate and formate species on the support, whose signals may overgrow also an underlying H_2O peak. The amount of side products/reaction intermediates quickly reaches a steady-state equilibrium value; their peak intensities do not increase significantly after 30 min [56]. On the other hand, experiments exposing a carbonate-covered Au/Fe_2O_3 catalyst to a H_2/O_2-containing atmosphere showed the conversion of carbonates into thermally less stable bicarbonates, which was explained by a reaction with water formed in that atmosphere [17]. On Au/TiO_2, where the tendency for carbonate formation is much lower, the H_2O-induced conversion and decomposition of the carbonate species appear to be fast enough to keep the level of adsorbed carboxylate/carbonate species low under steady-state conditions. Correspondingly, the H_2O signal dominates the carbonate region in the IR spectra.

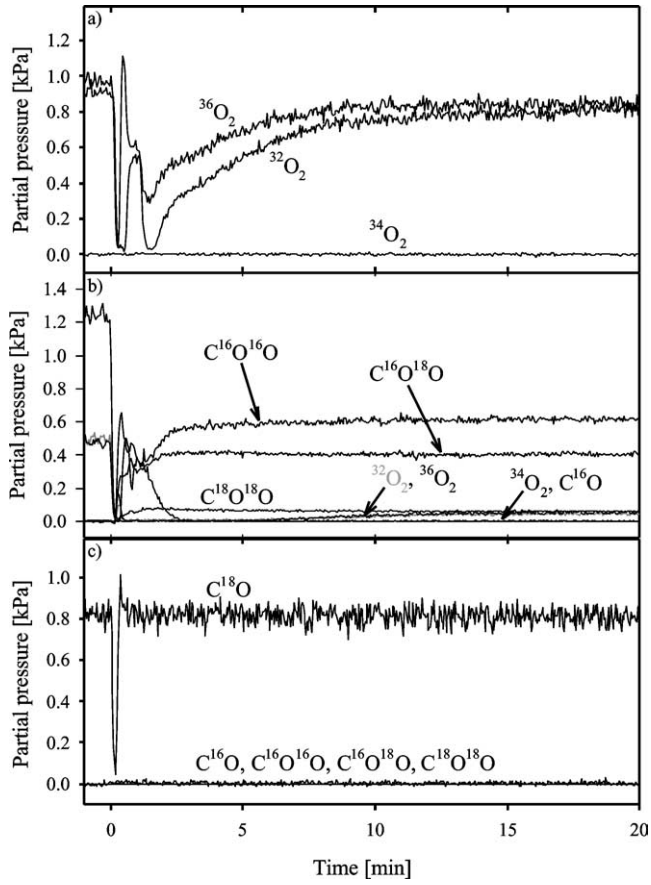

Fig. 8. Isotope-exchange experiments using $^{18}O_2$ and $C^{18}O$. All experiments were carried out at a flux of 40 N ml/min at 80 °C. (a) Introduction of 0.9 kPa $^{32}O_2$ and 1.0 kPa $^{36}O_2$ to the diluted Au/TiO_2(C) catalyst (diluted 1:15 with α-Al_2O_3, 100.7 mg). (b) CO oxidation when 0.5 kPa $^{32}O_2$ and $^{36}O_2$ and 1.2 kPa $C^{16}O$ are introduced to diluted catalyst Au/TiO_2(C) (1:15 with α-Al_2O_3, 100.7 mg). (c) Introduction of $C^{18}O$ in N_2 to diluted catalyst Au/TiO_2(C) (1:5 with α-Al_2O_3, 74.6 mg).

3.3. IMR-MS measurements with isotope-labeled gases

In this section we describe experiments using isotope-labeled reactants which were performed to get more direct information on the reaction mechanism on this catalyst. In order to test whether the interaction of O_2 with the catalyst under reaction conditions results in isotope scrambling, we introduced a mixture of $^{16}O_2$ and $^{18}O_2$ to a dilute Au/TiO_2 catalyst (see Fig. 8a). The catalyst had been calcined at 400 °C before the experiment. As shown in Fig. 8a, no $^{16}O^{18}O$ was formed, neither during the reaction under those conditions (Fig. 8a) nor during a subsequent desorption spectrum, when the sample was heated up to 300 °C (spectrum not shown). This rules out reaction pathways involving dissociative adsorption and the formation of adsorbed O_{ad}, which could undergo recombinative desorption, on this catalyst. Our findings are consistent with results from Iwasawa and co-workers [29,57], who studied the room temperature

adsorption–desorption behavior of a similar isotope-labeled O_2 gas mixture on a Au/TiO_2 catalyst prepared from organic gold and titanium precursors, and from a study of the transient O_2 adsorption/desorption behavior by Olea et al. [58]. It also agrees with observations in previous studies in on a Au/Fe_2O_3 catalyst, where equally no isotope scrambling, i.e., no $^{16}O^{18}O$ formation, was observed [5,59].

The evaluation of the temporal evolution of the O_2 signals, after switching from the bypass mode (O_2 flow through the bypass) to the reactor mode (O_2 flow through the reactor), is complicated by an experimental artifact. An initial peak, which is either positive-going ($^{18}O_2$) or negative-going ($^{16}O_2$), depending on the exact conditions, and which is introduced by the switching of the gas lines, prevents the quantitative evaluation of the first 1.5 min. Essentially, upon switching from bypass to reactor mode, at $t = 0$, the O_2 partial pressures drop to 0 kPa ($^{18}O_2$) or to about 0.3 kPa ($^{16}O_2$), respectively. Subsequently, both signals increase slowly to about 0.8 kPa, which is close to the steady-state value determined in the bypass measurements. A semilogarithmic plot of the O_2 signals during the slow increase shows that these follow first-order kinetics most of the time, with time constants of about 3.2×10^{-3} s^{-1} ($^{16}O_2$) and 1.9×10^{-3} s^{-1} ($^{18}O_2$), respectively. The initial drop and the subsequent slow increase of both O_2 signals during the first 10 min indicate an initial O_2 consumption before reaching steady-state conditions. A more detailed study of the transient reaction and the amount of adsorbed oxygen behavior is in progress.

Similar observations of significant O_2 consumption of a Au/TiO_2 catalyst upon exposure to O_2 had been made for catalysts prepared by impregnation and subsequent reductive pretreatment, which had considerably larger Au nanoparticles [26], as well as for Au/Fe_2O_3 [5]. This effect was explained by molecular adsorption of O_2 on the oxide support, most likely on defect sites.

In a second experiment we passed a gas mixture containing $C^{16}O$ (1.2 kPa), $^{16}O_2$ (0.5 kPa), and $^{18}O_2$ (0.5 kPa) over the Au/TiO_2 catalyst at 80 °C (see Fig. 6b). The activity of the catalyst was sufficient to maintain almost complete conversion over the entire time, as indicated by the negligible $C^{16}O$ intensity. The main oxidation product was $C^{16}O_2$, followed by $C^{16}O^{18}O$ (final intensity 65% of the $C^{16}O_2$ intensity), and very little $C^{18}O_2$ (steady-state concentrations: $C^{16}O_2$:$C^{16}O^{18}O$:$C^{18}O_2$ = 10:7:1). No $^{16}O^{18}O$ could be detected in this experiment, neither during the reaction (Fig. 8b) nor afterward, when the sample was heated to 300 °C (spectrum not shown), indicating that also under reaction conditions free O_{ad} species are not present or only in nondetectable amounts. Because of fluctuations in the O_2 signals during the first 2 min, which may be due to hot-spot formation, we did not attempt a quantitative evaluation of the time dependence.

Rather similar results, with an isotope distribution for the CO_2 product of $C^{16}O_2$:$C^{16}O^{18}O$:$C^{18}O_2$ = 9.7:6:1, were obtained by Liu et al. for CO oxidation on their Au/TiO_2 catalyst [29]. By flowing labeled CO_2 over the catalyst, these authors had also shown, however, that CO_2 can exchange oxygen with the Au/TiO_2 catalyst. Therefore, the observation of $C^{18}O_2$ cannot be taken as proof for a reaction mechanism proceeding via a carbonate intermediate, where the latter is formed by reaction between CO and an (activated) molecular oxygen species. In the latter case and without oxygen exchange between catalyst and CO_2 the expected isotope distribution would have been 3:2:1, provided that the decomposition of the CO_3 species occurs randomly with similar probabilities. Hence the relative amount of $C^{18}O_2$ would have been significantly higher. On the other hand, in a Langmuir–Hinshelwood reaction mechanism one would expect equal amounts of $C^{16}O_2$ and $C^{16}O^{18}O$. Taking into account the possibility of subsequent oxygen exchange between CO_2 and the TiO_2 substrate and assuming steady-state conditions, the amount of $C^{18}O_2$ should be identical to double the "loss" of $C^{16}O^{18}O$ ($2C^{16}O^{18}O \leftrightarrow C^{16}O_2 + C^{18}O_2$), i.e., to one-third of the difference between $C^{16}O_2$ and $C^{16}O^{18}O$. This is exactly the case in the present measurements, and also in the experiments reported by Liu et al. [29]. If we assume that the reactivities of $^{16}O_2$ and $^{18}O_2$ for CO_2 formation are similar, it is not possible under steady-state conditions to reach such a ratio in a reaction mechanism proceeding via a carbonate intermediate. (For carbonate decomposition without subsequent oxygen exchange (ratio of isotopomers $C^{16}O_2$:$C^{16}O^{18}O$:$C^{18}O_2$ = 3:2:1), the $C^{18}O_2$ signal should be equal to the full difference between the two other CO_2 signals, and additional oxygen exchange cannot lead to the experimental value.) Therefore, this result supports a mechanism with equal amounts of the two isotopomers $C^{16}O_2$ and $C^{16}O^{18}O_2$ being produced in the reaction, and subsequent oxygen exchange. From the time dependence of the three CO_2 signals it is clear that the equilibration between gas-phase CO_2 composition and surface composition must be rather fast, on the order of about a minute at most, which agrees with findings of Liu et al. upon interaction at room temperature CO_2 interaction with a Au/TiO_2 catalyst [29], considering the different reaction temperatures. Since oxygen exchange was also found in the absence of gaseous O_2, the exchange reaction must involve other oxygen species than the "active" molecular O_2 species, most likely lattice oxygen. Finally, it is interesting to note that these results contrast the behavior on Au/Fe_2O_3, where no $C^{18}O_2$ formation was observed [5].

In the last experiment we tested whether the interaction of CO with the Au/TiO_2 catalyst leads to oxygen exchange, by passing $C^{18}O$ over it (Fig. 8c). From the absence of any detectable amounts of $C^{16}O$ this can clearly be ruled out. Also, we do not see any CO_2 formation. Hence significant contributions from a Mars–van Krevelen-type mechanism [60] can equally be ruled out. Also these results equals the behavior reported by Liu et al. [29]. The close similarity in the reaction behavior between their Au/TiO_2 catalyst and our DP-prepared Au/TiO_2 catalyst leads to the conclusion that there are no basic differences in the reaction mechanism on these rather differently prepared Au/TiO_2 catalysts.

4. Summary

We have investigated the CO oxidation behavior and in particular the effect of H_2 on this reaction on a highly active Au/TiO_2 catalyst, prepared via a novel synthesis and pretreatment procedure, which involves a modified deposition–precipitation synthesis process. Following a previous report on the CO oxidation activity and deactivation/stability of this catalyst [23], this paper focuses on kinetic and mechanistic aspects of the CO oxidation reaction, the influence of H_2 on the reaction, and the interaction of CO with that catalyst, both in an inert and in a reactive atmosphere and in the absence and in the presence of H_2. Based on kinetic measurements, in situ IR spectroscopic measurements and isotope-labeling experiments we derive the following conclusions.

CO interaction with this catalyst, in an inert atmosphere in the absence of H_2 and at around 80 °C, results in on-top CO adsorption on the Au nanoparticles, with a peak at 2112 cm^{-1}, which red-shifts with increasing coverage to 2108 cm^{-1}. This resembles observations on Au/TiO_2 catalysts prepared and conditioned via other procedures. Furthermore, formate, carboxylate, and carbonate species are formed, which are identified by characteristic vibrations in the 1300–1700 cm^{-1} regime and, for formates, by their C–H vibrations between 2800 and 3000 cm^{-1}. The presence of H_2 has a pronounced effect on the interaction of CO with the Au/TiO_2 catalyst. The C–O stretch frequency is slightly red-shifted by 3 cm^{-1}, which results either from charge donation from the partly reduced substrate or, preferably, from indirect interaction of H and CO species coadsorbed on the Au nanoparticles. More important, with increasing reaction time it leads to the slow appearance of a new, strongly asymmetric absorption band with its maximum at 2032 cm^{-1}, which finally replaces the original peak at 2107 cm^{-1}, together with an increasing hydroxylation of the support. Based on the constant position and shape of this peak we favor an explanation where this new feature results from an H/CO adsorption complex rather than from charge transfer from the increasingly reduced TiO_2 substrate to the Au nanoparticles. In addition, the presence of H_2 inhibits formate or carbonate formation. In a reactive H_2-free atmosphere, in the presence of O_2, the formation of formates and in particular carbonates is considerably enhanced, which is held responsible for the decay of the CO oxidation activity with time. In the H_2-rich reactive atmosphere the new, asymmetric peak described above is not observed. On the other hand, formate/carbonate formation is still inhibited.

A pronounced effect of the H_2 coreactant is observed also in the kinetic measurements. In the temperature and pressure range investigated the reaction order for CO is almost doubled, from about 0.35 to about 0.9, while the O_2 reaction order is hardly affected and remains at about 0.35. This goes along with a reduced activity at all but the highest CO partial pressures investigated (1–1.5 kPa). The positive CO reaction order agrees well with the results of the IR CO adsorption measurements, where the amount of adsorbed CO was found to rise with the CO partial pressure in the gas mixture. We explain the reduced CO oxidation activity by the parallel adsorption and reaction of hydrogen, which competes for the reactive oxygen species. This in combination with the low O_2 reaction order points to the existence of a rate-limiting step between O_2 adsorption and oxidation reaction.

The selectivity for CO oxidation in the H_2-rich atmosphere depends strongly on the CO partial pressure, decaying from 57% at 1.5 kPa and 80 °C to 1.5% at 0.03 kPa. It is largely determined by the change in CO oxidation activity, while the H_2 oxidation rate changes little. Similar effects are observed upon temperature variation; e.g., a temperature increase from 40 to 80 °C reduces the selectivity from 64 to 40% at 1 kPa CO.

Experiments with isotope-labeled gases showed that no O_2 isotope scrambling occurs upon exposure to a mixture of $^{16}O_2$ and $^{18}O_2$, in agreement with previous findings for other Au/TiO_2 catalysts. O_2 isotope scrambling is also not observed under reaction conditions, indicating that the second O atom remaining after the reaction step cannot recombine with another, similar O adatom and desorb, but leaves the surface via reaction. The ratio of CO_2 isotopomers formed upon reaction with a mixture of $^{16}O_2$ and $^{18}O_2$ points to a reaction mechanism proceeding via a Langmuir–Hinshelwood process, with subsequent oxygen exchange between CO_2 and TiO_2 support process, rather than to the decomposition of a carbonate intermediate as major reaction path. Finally, transient experiments with $C^{18}O$ demonstrate that (i) oxygen exchange between CO and TiO_2 substrate is inhibited and that (ii) reaction with lattice oxygen is not possible after depletion of the "active" adsorbed O_2 species. The latter observation rules out significant contributions from a Mars–van Krevelen reaction mechanism on this catalyst.

The above results lead to the proposal that (i) H_2 in the gas phase affects the CO oxidation by competing hydrogen adsorption on the Au nanoparticles and reaction with oxygen, resulting in a significantly higher CO reaction order, that (ii) interaction with H_2O, which is present in the process gas or formed upon reaction with H_2, increases the activity indirectly by reducing the steady-state concentration of reaction inhibiting formate/carbonate species, and that (iii) formate and carbonate species formed during reaction represent (reaction inhibiting) side products, but do not take part in the reaction as reaction intermediate, at least not under the present reaction conditions.

Acknowledgment

We gratefully acknowledge financial support by the Deutsche Forschungsgemeinschaft within the Priority Programme 1091 (Be 1201/9-3).

References

[1] M. Haruta, Catal. Surv. Jpn. 1 (1997) 61.
[2] G.C. Bond, Catal. Rev.-Sci. Eng. 41 (1999) 319.
[3] M. Haruta, M. Daté, Appl. Catal. A 222 (2001) 427.
[4] M. Haruta, CATTECH 6 (2002) 102.
[5] M.M. Schubert, S. Hackenberg, A.C. van Veen, M. Muhler, V. Plzak, R.J. Behm, J. Catal. 197 (2001) 113.
[6] F. Boccuzzi, A. Chiorino, J. Phys. Chem. B 104 (2000) 5414.
[7] G.R. Bamwenda, S. Tsubota, T. Nakamura, M. Haruta, Catal. Lett. 44 (1997) 83.
[8] M. Haruta, S. Tsubota, T. Kobayashi, H. Kageyama, M.J. Genet, B. Delmon, J. Catal. 144 (1993) 175.
[9] Y. Iizuka, H. Fujiki, N. Yamauchi, T. Chijiiwa, S. Arai, S. Tsubota, M. Haruta, Catal. Today 36 (1997) 115.
[10] A.I. Kozlov, A.P. Kozlova, H. Liu, Y. Iwasawa, Appl. Catal. A 182 (1999) 9.
[11] J.-D. Grunwaldt, A. Baiker, J. Phys. Chem. B 103 (1999) 1002.
[12] F. Boccuzzi, A. Chiorini, M. Manzoli, P. Lu, T. Akita, S. Ichikawa, M. Haruta, J. Catal. 202 (2001) 256.
[13] M.M. Schubert, V. Plzak, J. Garche, R.J. Behm, Catal. Lett. 76 (2001) 143.
[14] M.J. Kahlich, M.M. Schubert, M. Hüttner, M. Noeske, H.A. Gasteiger, R.J. Behm, in: O. Savadogo, P.R. Roberge (Eds.), New Materials for Fuel Cells and Modern Battery Systems II, Ecole Polytechnique de Montreal, Montreal, 1997, pp. 642–653.
[15] M.M. Schubert, M.J. Kahlich, H.A. Gasteiger, R.J. Behm, J. Power Sources 84 (1999) 175.
[16] Y.-F. Han, V. Plzak, M. Kinne, R.J. Behm, in: F.N. Büchi, G. Scherer, A. Wokaun (Eds.), Proc. 1st European Fuel Cell Forum, Luzern, 2001, pp. 393–396.
[17] M.M. Schubert, A. Venugopal, M.J. Kahlich, V. Plzak, R.J. Behm, J. Catal. 222 (2004) 32.
[18] Y.-F. Han, V. Plzak, M. Kinne, R.J. Behm, Submitted for publication.
[19] S. Gottesfeld, T.A. Zawodzinski, in: R.C. Alkire, H. Gerischer, D.M. Kolb, C.W. Tobias (Eds.), Advances in Electrochemical Science and Engineering, vol. 5, Wiley–VCH, Weinheim, 1997.
[20] D.P. Wilkinson, D. Thompsett, in: O. Savadogo, P.R. Roberge (Eds.), Materials and Approaches for CO and CO_2 Tolerance for Polymer Electrolyte Membrane Fuel Cells, Ecole Polytechnique de Montreal, Montreal, 1997, pp. 266–285.
[21] D.L. Trimm, Z.I. Önsan, Catal. Rev. 43 (2001) 31.
[22] J.M. Zalc, V. Sokolovskii, D.G. Loeffler, J. Catal. 206 (2002) 169.
[23] B. Schumacher, V. Plzak, M. Kinne, R.J. Behm, Catal. Lett. 89 (2003) 109.
[24] S.D. Lin, M.A. Bollinger, M.A. Vannice, Catal. Lett. 17 (1993) 245.
[25] M.A. Bollinger, M.A. Vannice, Appl. Catal. B 8 (1996) 417.
[26] N.J. Ossipoff, N.W. Cant, Top. Catal. 8 (1999) 161.
[27] T.V. Choudhary, C. Sivadinarayana, C.C. Chusuei, A.K. Darye, J.P. Fackler, D.W. Goodman, J. Catal. 207 (2002) 247.
[28] F. Boccuzzi, A. Chiorino, M. Manzoli, Surf. Sci. 502–503 (2002) 513.
[29] H. Liu, A.I. Kozlov, A.P. Kozlova, T. Shido, K. Asakura, Y. Iwasawa, J. Catal. 185 (1999) 252.
[30] V. Plzak, J. Garche, R.J. Behm, Eur. Fuel Cell News 10 (2003) 8.
[31] M.J. Kahlich, H.A. Gasteiger, R.J. Behm, J. Catal. 171 (1997) 93.
[32] P.B. Weisz, Chem. Eng. Progr. Ser. 55 (1959) 29.
[33] I.M. Hamadeh, P.R. Griffiths, Appl. Spectrosc. 41 (1987) 682.
[34] H. Schubert, U. Guntow, K. Hofmann, R. Schlögl, Fresenius J. Anal. Chem. 356 (1996) 127.
[35] M.J. Kahlich, H.A. Gasteiger, R.J. Behm, J. Catal. 182 (1999) 430.
[36] R.M. Torres Sanchez, A. Ueda, K. Tanaka, M. Haruta, J. Catal. 168 (1996) 125.
[37] R.J.H. Grisel, K.-J. Weststrate, A. Goossens, M.W.J. Craje, A.M. van der Kraan, B. Nieuwenhuys, Catal. Today 72 (2002) 123.
[38] H. Sakurai, A. Ueda, T. Kobayashi, M. Haruta, Chem. Commun. 271 (1998).
[39] F. Boccuzzi, A. Chiorino, S. Tsubota, M. Haruta, J. Phys. Chem. 100 (1996) 3625.
[40] J.-D. Grunwaldt, M. Maciejewski, O.S. Becker, P. Fabrizioli, A. Baiker, J. Catal. 186 (1999) 458.
[41] J. France, P. Hollins, J. Electr. Spectrosc. Rel. Phenom. 64/65 (1993) 251.
[42] C. Ruggiero, P. Hollins, J. Chem. Soc., Faraday Trans. 92 (1997) 4829.
[43] P. Hollins, Surf. Sci. Rept. 16 (1992) 51.
[44] G. Busca, J. Lamotte, J.-C. Lavalley, V. Lorenzelli, J. Am. Chem. Soc. 109 (1987) 5197.
[45] F. Boccuzzi, S. Tsubota, M. Haruta, J. Electr. Spectrosc. Rel. Phenom. 64–65 (1993) 241.
[46] L.-F. Liao, D.-L. Lien, D.-L. Shieh, M.-T. Chen, J.-L. Lin, J. Phys. Chem. B 106 (2002) 11240.
[47] C.-C. Chuang, W.-C. Wu, M.-C. Huang, I.-C. Huang, J.-L. Lin, J. Catal. 185 (1999) 423.
[48] G.C. Bond, D.T. Thompson, Gold. Bull. 33 (2000) 41.
[49] G. Martra, Appl. Catal. A 200 (2000) 275.
[50] M.I. Zaki, G. Kunzmann, B.C. Gates, H. Knözinger, J. Phys. Chem. 91 (1987) 1486.
[51] F. Boccuzzi, A. Chiorino, M. Manzoli, Surf. Sci. 454–456 (2000) 942.
[52] M. Jakob, H. Levanon, P.V. Kamat, Nano Lett. 3 (2003) 353.
[53] B.E. Koel, D.E. Peebles, J.M. White, Surf. Sci. 125 (1983) 709.
[54] B.E. Koel, D.E. Peebles, J.M. White, Surf. Sci. 125 (1983) 739.
[55] F. Boccuzzi, A. Chiorino, S. Tsubota, M. Haruta, Shokubai (Catal. Catal.) 38 (1996) 422.
[56] M.M. Schubert, PhD dissertation, University of Ulm, 2000.
[57] M. Olea, M. Kunitake, T. Shido, Y. Iwasawa, Phys. Chem. Chem. Phys. 3 (2001) 627.
[58] M. Olea, M. Kunitake, T. Shido, K. Asakura, Y. Iwasawa, Bull. Chem. Soc. Jpn. 74 (2001) 255.
[59] H. Liu, A.I. Kozlov, A.P. Kozlova, T. Shido, Y. Iwasawa, Phys. Chem. Chem. Phys. 1 (1999) 2851.
[60] P. Mars, D.W. van Krevelen, Chem. Eng. Sci. 3 (1954) 41.
[61] N.W. Cant, N.J. Ossipoff, Catal. Today 36 (1997) 125.